



# Strategies for Minimizing Stray Losses in Power Transformers: Effects of Shield Material and Placement

Mahsa Taghilou<sup>1</sup> and Mojtaba Mirsalim<sup>1\*</sup>

## Abstract

A transformer is a vital component of the power grid infrastructure as it facilitates efficient transmission, distribution, and utilization of electrical energy, and ensures reliable and uninterrupted power supply to consumers. As the demand for electricity in a power grid increases, additional transformers with higher ratings may be required to handle the increased load. Therefore, the reduction of losses in power transformers is essential for optimizing energy efficiency, reducing costs, and maintaining a reliable power grid. Stray loss which is 20-25% of the total load loss of the transformer, can affect power quality by introducing harmonics into the power grid. Stray losses also increase the temperature, and cooling requirement for the transformer. In addition to the power grid's cost and performance, the transformer's lifetime is also important, which ultimately depends on the amount of losses. Therefore, to compromise between the cost and performance and guarantee losses, it should be reduced. In reducing stray losses, shielding is an effective technique that generates opposing fields to the stray flux or establishes a path with lower reluctance. In this study, the three-dimensional finite element method (FEM) is employed to accurately assess the stray losses in the structural components of a 250 MVA power transformer. Various factors, including the choice of materials (ferromagnetic and copper) and the strategic placement of shields, are considered to minimize energy losses and enhance the overall efficiency of the transformer.

**Keywords:** Power Transformer, Stray Loss, Leakage Flux, Shield Material, Shield Placement.

*Received Date: 2025-01-05; Revised Date: 2025-03-02; Accepted Date: 25-09-29.*

## 1. INTRODUCTION

The power transformer is a high-efficiency electrical device that links between a power plant and utilization. Today, the use of energy-efficient power transformers is becoming more important due to the cost of energy resources from an economic point of view. Therefore, manufacturers aim to achieve transformer efficiencies exceeding 99%—for instance, in units rated at 250 MVA—to enhance their competitiveness in the sales market [1]. It is generally observed that larger electromagnetic apparatuses can attain higher efficiency due to improved cooling mechanisms, reduced losses from enhanced materials, and optimized designs. According to IEC 60076-21, the load losses in power transformers include  $RI^2$  loss in the current carrying parts (windings, leads, busbars, and bushings), eddy losses in conductors due to eddy currents, circulating currents (if any) in parallel windings or parallel winding strands, and stray loss induced by leakage flux in the tank, core clamps, or other structural parts. Stray losses arise from the stray components of the magnetic field that do not couple with the primary and secondary windings.

These stray losses can be further divided into two main groups: those associated with the copper components and those related to the steel components. Additionally, while there is a small amount of stray loss in the iron core, it is typically negligible due to the laminated design of the core. Stray losses which depend on permeability, resistivity, and distance between the active part and structural parts of the transformer can cause thermal failure due to temperature rise [2]. According to IEEE C57.91, conductor and structural parts' maximum hotspot temperatures at nameplate operation, limit to 120°C and 140°C, respectively. The conductor hot spot is at the top of the coil which is the place of concentration of leakage fluxes [3]. If the flux density becomes too high, an excessive temperature rise affects the insulation system. Given that the standard life span of a transformer (7500 days) is based on the aging of insulation, even though the stray losses include only 20-25% of the total load loss of the transformer, it should be controlled properly [4]. Proper design and construction techniques, including using magnetic and copper shields, can help minimize these losses and improve the overall efficiency of the transformer [5][6]. In [7] the ways to

<sup>1</sup>Department of Electrical Engineering, Amirkabir University of Technology, Tehran, Iran.  
Electrical Machines and Transformer Research Lab.  
\*Corresponding author, Email: mojtaba\_mirsalim@yahoo.com, mirsalim@aut.ac.ir  
© 2025 Niroo Research Institute, All rights reserved.

control stray losses outside of the winding by increasing the magnetic resistance, using active (copper and aluminum) and passive (silicon steel sheets) magnetic shields have been presented. Magnetic shields on the transformer tank wall can be horizontal, vertical, or combined. By using horizontal shunts, the total weight of the shunts is reduced by 25% when compared with the vertical shunts while stray losses are almost the same [8]. The magnetic shunt material and geometry can reduce stray losses as much as possible. The results presented in [9] indicate that non-oriented electrical steel (NOES) shunts reduce material, manufacturing, labor, and energy costs; however, they increase power losses and weight. The influence of magnetic shunt geometry on the transformer leakage field is presented in [10]. To make the simulation results more accurate, [11] considers the conductivity temperature coefficient.

This paper, an extended version of our work published in the 2023 3rd International Conference on Electrical Machines and Drives (ICEMD), IEEE [12], introduces a pioneering comparative analysis focused on the placement of high-permeability magnetic shields to effectively reduce stray losses in a 250 MVA three-phase, three-legged power transformer. Unlike previous studies, this research not only examines the strategic positioning of these shields on critical structural components, such as tank walls and yoke beams, but also investigates the influence of shield material—specifically copper versus steel—on their placement efficacy. The innovative aspect of this study lies in its comprehensive approach, utilizing advanced modeling techniques through COMSOL Multiphysics to create a detailed three-dimensional geometry of the transformer. By employing surface impedance boundary conditions (IBC) and magnetization curves for accurate calculations, the paper provides valuable insights into how varying the materials and placements of shields can lead to significant reductions in stray losses.

## 2. FINITE ELEMENT MODEL

This section explains the 3D geometry modeling of the power transformers based on the finite element method and the stray loss calculation of structural parts and shields. Fig.1 shows the 3D geometry and front view of overall structure of the 250 MVA power transformer, and Tables I and II show the power transformer's technical characteristics and material properties, respectively. The model comprises a core, windings, tank walls, structural parts (yoke beams, flitch plates), and shields. Tank and yoke shields are modeled as parallel to the tank walls and perpendicular to the yoke beams, respectively. The windings are modeled as a solid cylinder. The geometry of the transformer is meticulously created in COMSOL, where the materials utilized in the model are defined with their relevant properties, such as electrical conductivity, magnetic permeability, and any nonlinear B-H curve data.

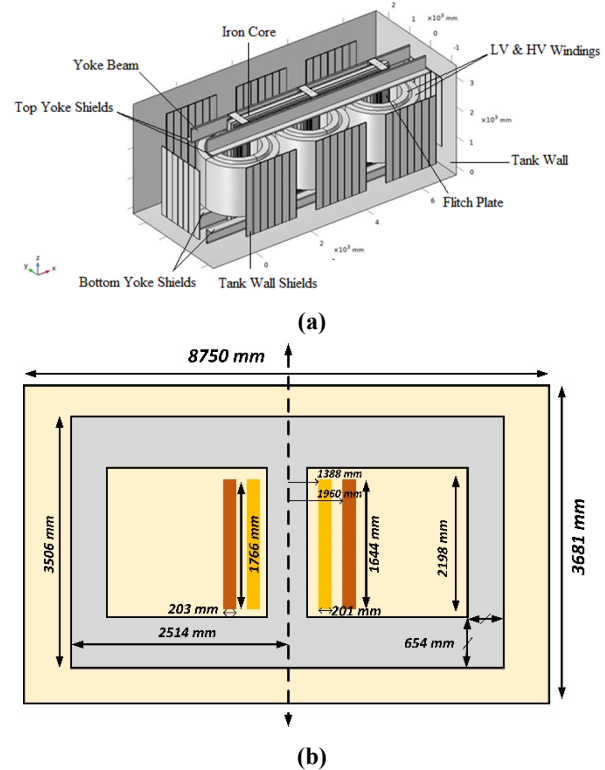


Fig.1. Geometric representation of the modeling framework, a) 3D geometry, b) Front view

TABLE. 1. Material properties of model

Components	Material	$\mu_r$	$\sigma$ (S/m)
Oil	oil	1	10
Winding	Copper	1	0.001
Iron Core	HiB	$10 \times 10^3$	0.001
Shields (Passive)	HiB	$10 \times 10^3$	0.001
Shields (Active)	Copper	0.99	$5.96 \times 10^7$
Tank Wall	St-37	500 – 700	0.001
Yoke Beam	St-37	500 – 700	0.001
Flitch Plate	St-37	500 – 700	0.001

TABLE. 2. Technical characteristics of model

Transformer rating	250 MVA
Impedance (normal tap)	15.5%
Phase number	3
Nominal low voltage current (rms)	436 A
Nominal high voltage current (rms)	190 A
High voltage / Low voltage	345/230 kV
$N_{HV} / N_{LV}$	117/512
Cooling system	ONAF
Operating frequency	50 Hz

To facilitate this process, the "Magnetic Fields" interface is employed to solve Maxwell's equations, which enables the simulation of magnetic field distributions and the calculation of stray flux. These equations are discretized and

subsequently solved for each finite element within the problem domain, ensuring accurate representation of the physical phenomena. Furthermore, during the model setup in COMSOL, boundary conditions are carefully defined to influence the behavior of the magnetic fields at interfaces between different materials as well as at external boundaries. The study is conducted in the frequency domain, wherein alternating current (AC) sources are applied, and the induced eddy currents are calculated based on the time-varying magnetic fields. A mesh of finite elements is generated by the software according to the specified dimensions, allowing for a comprehensive solution of Maxwell's equations that describe the intricate interaction of electric and magnetic fields. Maxwell's equations composed of four partial differential equations are as follows:

$$\nabla \cdot D = \rho \tag{1}$$

$$\nabla \cdot B = 0 \tag{2}$$

$$\nabla \times E = -\partial B/\partial t \tag{3}$$

$$\nabla \times H = J + \partial D/\partial t \tag{4}$$

The primary objective of electromagnetic (EM) loss is to generate heat, which can be either intentional or an undesired effect. The standard model for loss is derived from resistive heating. In the context of induction heating, the focus is on the heating effects caused by induced currents and magnetic losses. In the frequency domain, the heat source is incorporated through specific equations.

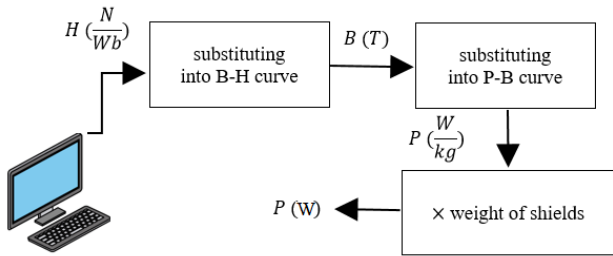


Fig. 2. The block diagram of loss calculation in tank and yoke shields

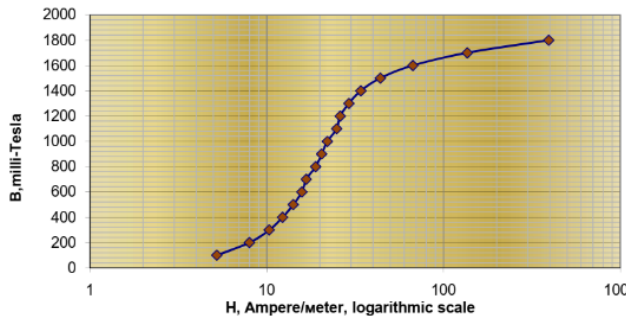


Fig. 3. The B-H curve of magnetic shields

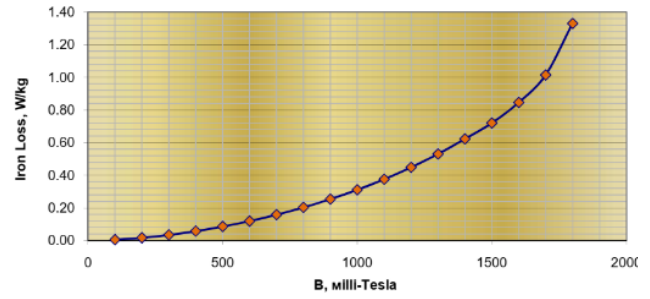


Fig. 4. The P-B curve of magnetic shields

For this analysis, key material properties that characterize loss include electrical conductivity ( $\sigma$ ) and magnetic permeability ( $\mu$ ). The expressions of the loss models are as follows:

$$Q_e = Q_{rh} + Q_{ml} \tag{5}$$

$$Q_{rh} = \frac{1}{2} Re(J \cdot E^*) \tag{6}$$

$$Q_{ml} = \frac{1}{2} Re(i\omega B \cdot H^*) \tag{7}$$

$$J = \sigma E \tag{8}$$

$$B = \mu_0 \mu_r H = \mu_0 (\mu_r' - j\mu_r'') H \tag{9}$$

### 2.1. Stray losses in structural parts

Eddy currents that lead to losses in power transformers depend on the thickness of structures. In the structural parts of the transformer, the skin depth (that is, the distance where the electromagnetic field has decreased by a factor  $e^{-1}$ ) is too small and the penetration depth is less than 1 mm due to their materials. [6]. Therefore, making fine mesh cutting all over them is time-consuming. The impedance boundary condition (IBC) provides a boundary condition that is useful at the boundary where the electromagnetic field penetrates only a short distance outside the boundary. The boundary condition approximates this penetration to avoid the need to include another domain in the model. The skin depth and the IBC are expressed in equations (10) and (11) as follows:

$$\delta = \sqrt{\frac{2}{\omega \mu \sigma}} \tag{10}$$

$$\sqrt{\frac{\mu_0 \mu_r}{\epsilon_0 \epsilon_r - j \frac{\sigma}{\omega}}} n \times H + E - (n \cdot E) n = (n \cdot E_s) n - E_s \tag{11}$$

### 2.2. Stray losses in tank and yoke shields

The shields play a crucial role in ensuring the proper function and reliability of power transformers by minimizing the electromagnetic interface. It can be achieved by using various techniques, including using metal plates or screens around the core and windings. Therefore, to mitigate the effects of leakage flux, the power transformers are designed with shields. If the leakage flux is strong enough, it can induce currents in the shielding

material and cause losses. To calculate the losses of tank and yoke shields considering saturation as shown in Figures 2 through 4, the maximum value of magnetic intensity,  $H_{max}$  is measured by COMSOL. By substituting  $H_{max}$  and magnetic field values, B into the B-H and P-B curves respectively, the loss value, P in Watt per kilogram obtained. This value contains hysteresis and eddy losses due to leakage flux. To obtain the P value in Watt, the weight of shields is calculated according to volume and volumetric density of them.

### 3. SIMULATION & RESULTS

This section explains the stray losses of structural parts and shields solved in COMSOL for time-harmonic electromagnetic analysis. To analyze the distribution of stray losses in the structural parts of the transformer, different combinations of tank and yoke shields are modeled as follows:

- Transformer without shields.
- Transformer with tank shields (Copper).
- Transformer with tank shields (HiB).
- Transformer with yoke shields (HiB).
- Transformer with both tank and yoke shields (HiB).

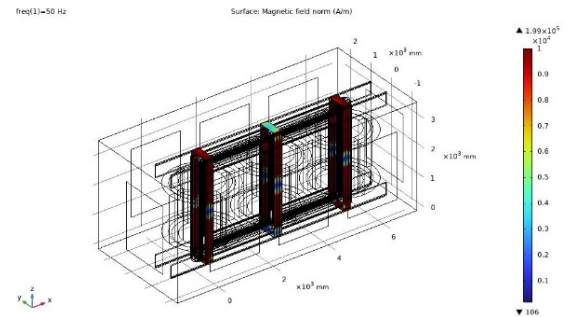


Fig. 7. Magnetic field distribution in flitch plates without shields

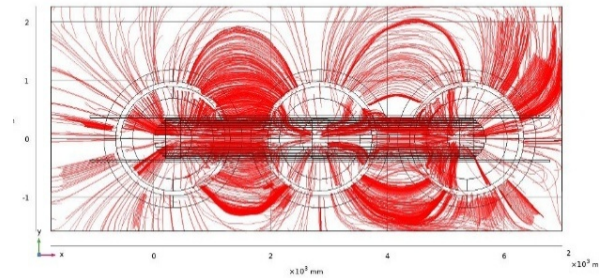


Fig. 8. Streamline of magnetic flux density without shields

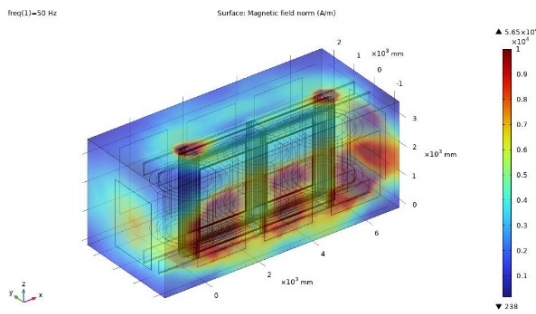


Fig. 5. Magnetic field distribution in tank walls without shields

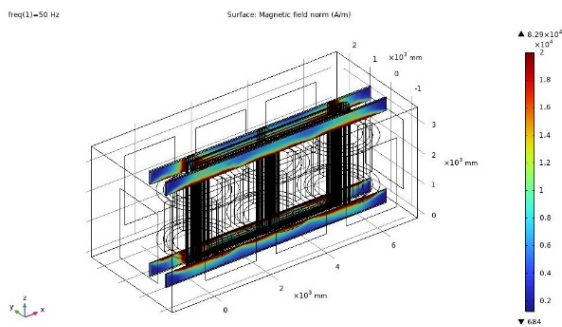


Fig. 6. Magnetic field distribution in yoke beam without shields

#### 3.1. Transformer without shields

In this case, from Fig.5, the stray loss in the tank walls is 163.5 kW which means that the surface of the tank walls deals with higher leakage flux. The stray losses in the yoke beams and flitch plates are 68 and 48.5 kW, as shown in Fig.6 and Fig.7, respectively. According to Fig.7 and Fig.8, the concentration of leakage fluxes in the flitch plates is too high compared with their dimensions. It is obvious that flitch plates near the windings, lead to local hot spots. Hence, the reduction of losses in flitch plates is vital. From Fig.6, it is observed that the concentration of leakage fluxes is in the bottom area of the top yoke beam and the top area of the bottom yoke beam.

#### 3.2. Transformer with tank shields (Copper)

In this case, the stray loss in the tank walls is measured at 160 kW, which is significantly lower compared to the previous case. The stray losses in the yoke beams, flitch plates, and tank shields are recorded as 50.7 kW, 45.8 kW, and 7.4 kW, respectively, as illustrated in Fig. 9 to Fig. 11. It can be observed that the losses in structural parts are lower in this scenario compared to the previous case, they still have the potential to create localized hot spots.

#### 3.3. Transformer with tank shields (HiB)

In this case, the stray loss in the tank walls is 69.2 kW demonstrating the importance of using magnetic shields. The stray losses in the yoke beams and flitch plates decrease to 47.2 and 39 kW, as shown in Fig.13 and Fig.14,

respectively, while the stray loss of the tank shield is 4 kW. From Fig.15 and Fig. 16, it is observed that the concentration of leakage fluxes in tank shields is on the side of them.

**3.4. Transformer with yoke shields (HiB)**

In this case, the stray loss in the tank walls is 86.7 kW, which is higher than the previous case. The stray losses in the yoke beams and flitch plates decrease to 35.4 kW and 25 kW, as shown in Fig.18 and Fig.19, respectively. The stray loss of the yoke shields is 34 kW, which is higher than the loss of tank shields in the previous case. The stray loss in flitch plates with yoke shields is lower than that with tank shields.

**3.5. Transformer with both tank and yoke shields (HiB)**

In this case, the stray loss in the tank walls is 30.7 kW, which is the lowest value compared with other previous cases. The stray losses in the yoke beams, flitch plates, tank shields, and yoke shields decrease

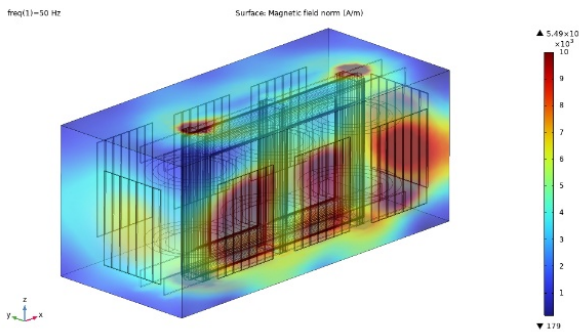


Fig. 9. Magnetic field distribution in tank walls with tank shields (Copper)

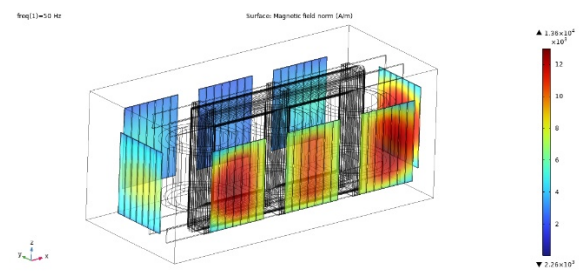


Fig. 10. Magnetic field distribution in tank shields (Copper)

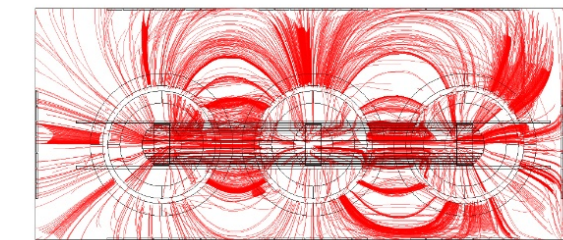


Fig. 11. Streamline of magnetic flux density with tank shields (Copper)

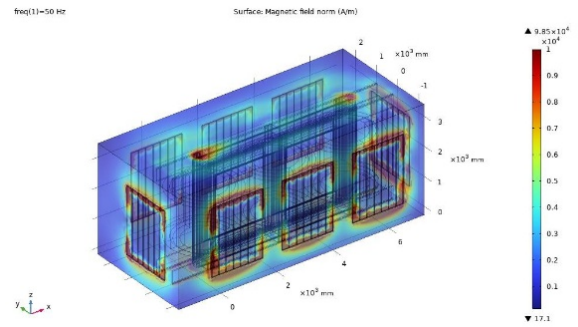


Fig. 12. Magnetic field distribution in tank walls with tank shields (HiB)

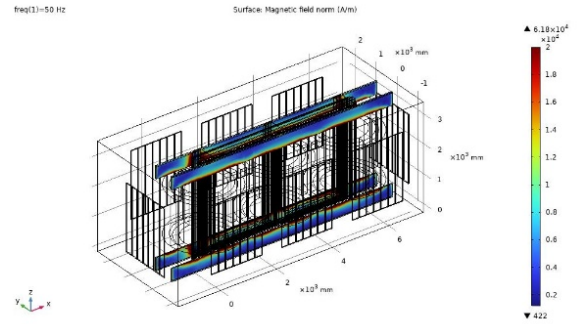


Fig. 13. Magnetic field distribution in yoke beam with tank shields (HiB)

to 22 kW, 20.8 kW, 3 kW, and 2.7 kW, as shown in Figs.22 to 25, respectively. Fig.26 shows that the concentration of leakage fluxes on the side of the tank shields is lower than in the third case. Losses of flitch plates in this case are lower than in the previous case but still can cause more local hot spots. Based on the results obtained from the first case, the stray losses of the transformer have been determined.

Based on the results obtained from the first case, the stray losses of the transformer have been determined. Given the significant increase in the magnetic field due to leakage flux in certain structural components of the transformer, the necessity of incorporating shields has been established. In the initial phase, after applying copper shields, it was observed that the loss values were somewhat reduced. However, this reduction was unacceptable due to the addition of copper components and their associated costs and performance. Furthermore, as observed, stray flux continues to penetrate the transformer structural components due to the low magnetic permeability of copper. Therefore, high-permeability ferromagnetic shields were employed to absorb these fluxes to reduce the losses across all transformer structures significantly. Given the superior performance of magnetic shields compared to copper shields, subsequent steps focused on placing these shields based on the flux distribution path within the tank, utilizing both tank walls and yoke shield types. Ultimately, by simultaneously employing these two types of magnetic shields, we observe the highest reduction in losses. Fig. 27

illustrates the differences between copper and magnetic shields in absorbing the stray flux. In the case of magnetic shields, due to their high magnetic permeability, a low reluctance path is created. Furthermore, because these shields are laminated, the eddy currents generated by the stray fields on the shields are significantly reduced compared to those on the walls of the tank, thereby preventing them from interacting with the tank walls of the transformer.

#### 4. DISCUSSION

In this research, different combinations of shields for reaching the minimum stray losses in the structural parts of the power transformer are modeled. Two kinds of shields are used to optimize the stray losses in the model. One is to place the tank shields (Copper/HiB) parallel to the tank walls and the other one (HiB) perpendicular to the yoke beams. It is important to note that the reason for selecting a yoke beam to apply the shields is the distribution of leakage fluxes. The yoke beams placed at the top and bottom of the winding are subjected to higher leakage fluxes. Therefore, by applying perpendicular shields to yoke beams, the low-reluctance path is created to absorb the fluxes that do not follow the intended path through the iron core and windings.

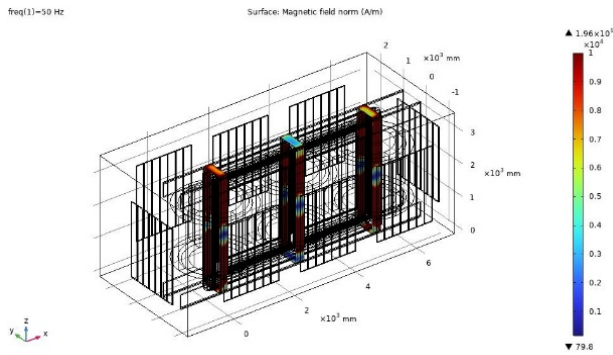


Fig. 14. Magnetic field distribution in flitch plates with tank shields (HiB)

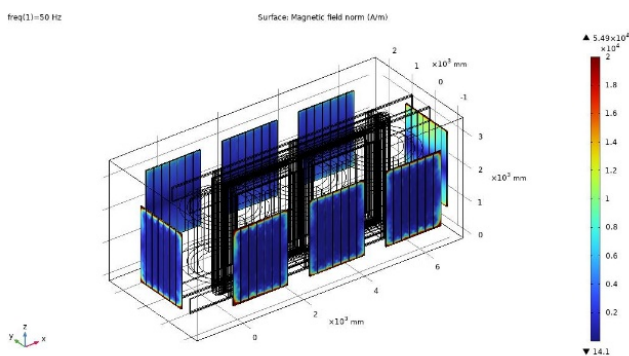


Fig. 15. Magnetic field distribution in tank shields (HiB)

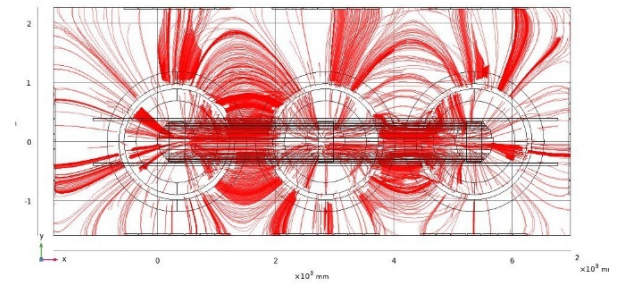


Fig. 16. Streamline of magnetic flux density with tank shields (HiB)

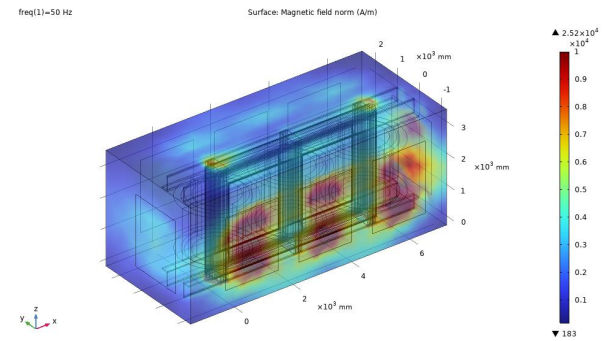


Fig. 17. Magnetic field distribution in tank walls with yoke shields (HiB)

Flitch plates cannot be used as a shield, because they are located directly in front of the core. If the leakage flux is so strong, it can induce more currents in the flitch plates, causing it to heat up and potentially degrade over time. This can lead to a decrease in the effectiveness of shields and an increase in the stray loss in the power transformer core more than before. The results obtained are shown in Table III. According to Fig.32, the general trend of changes in stray losses is downward. In case 2, the total stray loss of the power transformer and other losses are decreased, while the losses of tank shields are increased. In case 3, the application of magnetic shields has resulted in a greater loss reduction compared to the second case. In case 4, because of the application of the yoke shields, the total stray loss of the power transformer is increased by about 14%. Fig.32 shows that the losses of yoke shields in case 4 are higher than the tank shield losses in case 3 due to their placement. With the combination of tank and yoke shields, the total stray losses and other parts' losses were significantly reduced as shown in Table III. Although the flitch plate losses decrease, they cause more local hot spots. The distances between the core and the windings should be increased to control the temperature rise around the flitch plates and improve the cooling system. The cooling system operations will improve further by upgrading the cooling system to OFAF or ODAF and creating a cooling channel around the flitch plates. In case 5, the total stray loss is

decreased by about 70% which is more than in other cases, while the manufacturing cost of the power transformer will increase due to the use of both types of shields. Therefore, the design of the power transformer depends on a compromise between cost and performance.

The effective area of the shield significantly influences its ability to intercept stray magnetic fields; a larger shield can cover more of the transformer’s magnetic field, thereby reducing stray losses more effectively. However, if the shield is excessively large, it may introduce other issues such as increased weight or interference with adjacent components. Additionally, the shape of the shield can impact its overall effectiveness; for instance, a shield that closely conforms to the geometry of the transformer core tends to provide better shielding compared to a flat or poorly shaped shield.

Moreover, it is essential to note that the effectiveness of a magnetic shield diminishes with increasing distance from the source of the magnetic field, which is the transformer core. Consequently, placing the shield as close as possible to the source can maximize its shielding effect, thereby reducing stray losses more effectively.

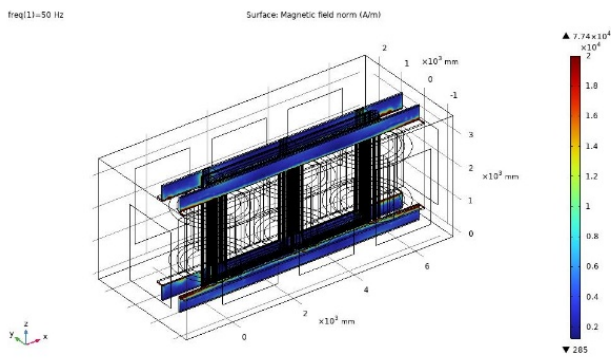


Fig. 18. Magnetic field distribution in yoke beam with yoke shields (HiB)

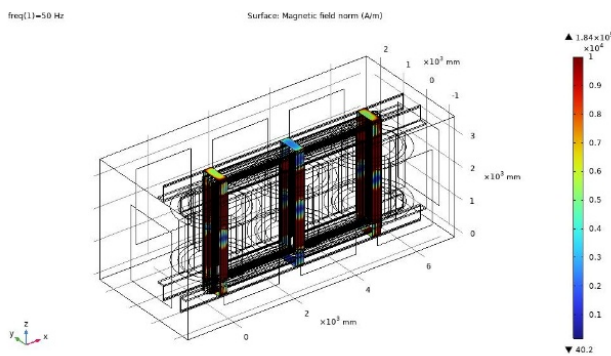


Fig. 19. Magnetic field distribution in flitch plates with yoke shields (HiB)

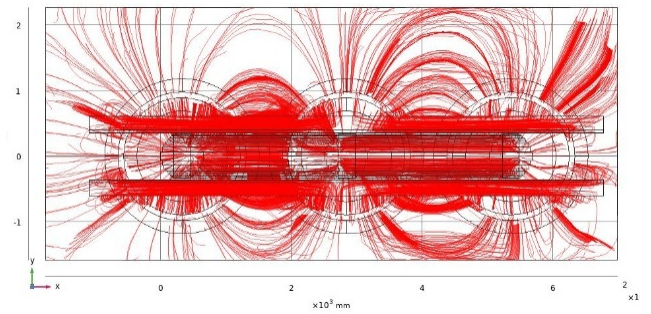


Fig. 20. Streamline of magnetic flux density with yoke shields (HiB)

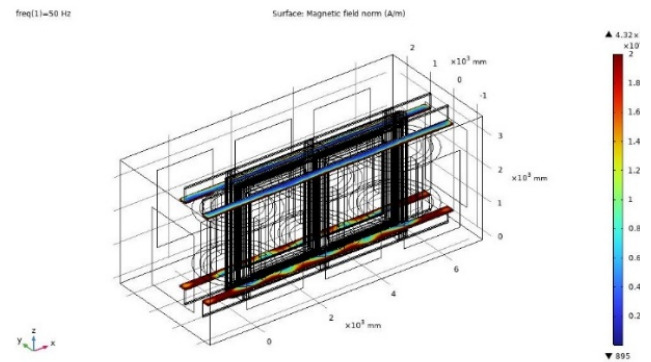


Fig. 21. Magnetic field distribution in yoke shields (HiB)

The maximum point values of the magnetic field over time at critical points without shields are illustrated in Figures 27 through 31. As previously mentioned, this concentration of the magnetic field arises from the stray fluxes in the upper part of the coils. Consequently, it can be observed from the Figures that during one complete cycle, these critical points exhibit the highest magnetic field intensity. In Fig. 31, the maximum magnetic field is observed in a complete cycle. As seen in Figures 28 to 30, the point of maximum field varies depending on the sinusoidal supply between the phases of the transformer.

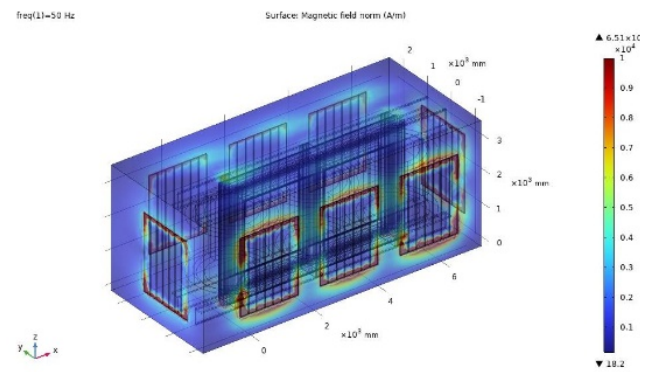


Fig. 22. Magnetic field distribution in tank walls with both HiB shields

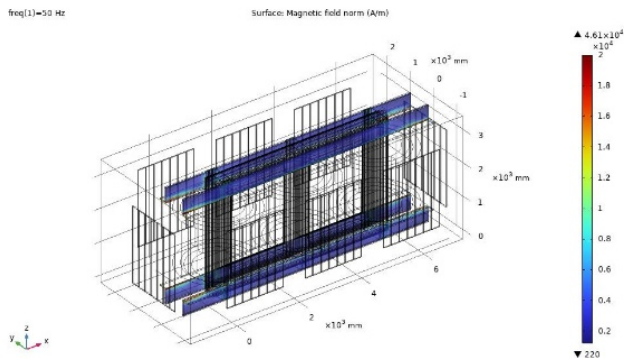


Fig. 23. Magnetic field distribution in yoke beam with both HiB shields

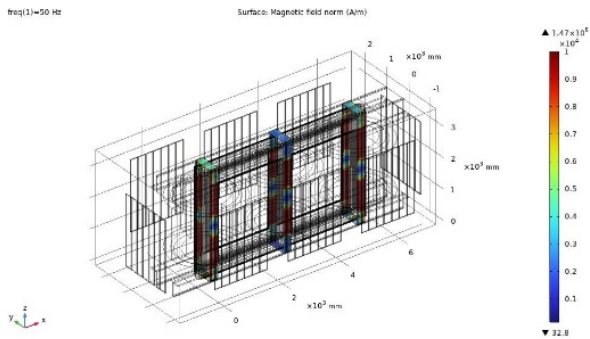


Fig. 24. Magnetic field distribution in fitch plates with both HiB shields

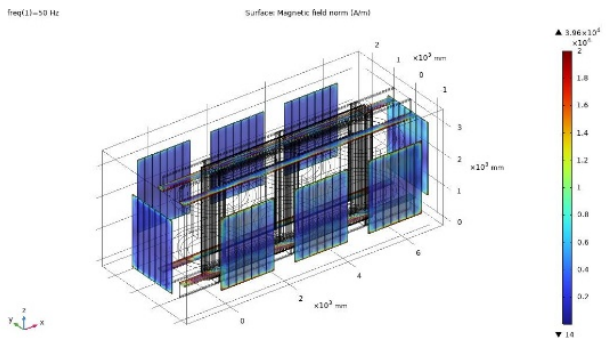


Fig. 25. Magnetic field distribution in both HiB shields

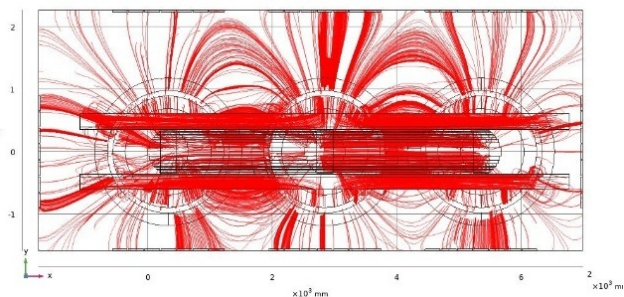


Fig. 26. Streamline of magnetic flux density with both HiB shields

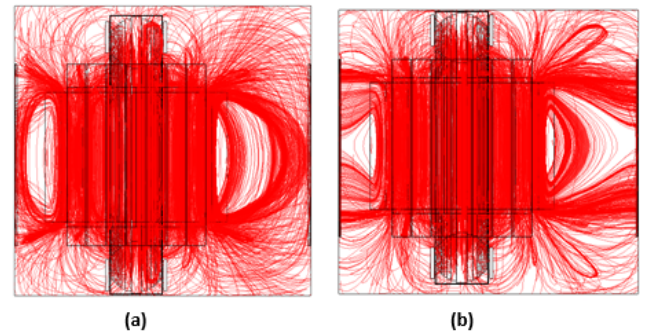


Fig. 27. Streamline of magnetic flux density with tank shields, a) Copper Shield b) Magnetic Shield

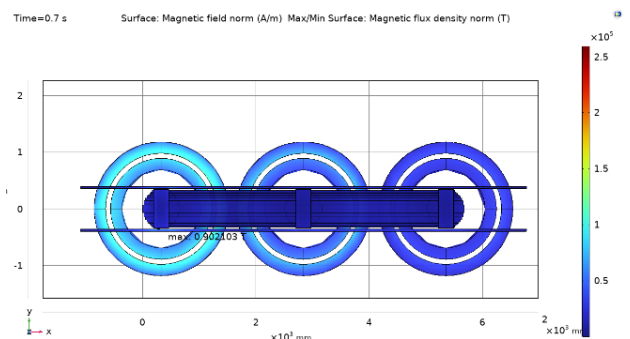
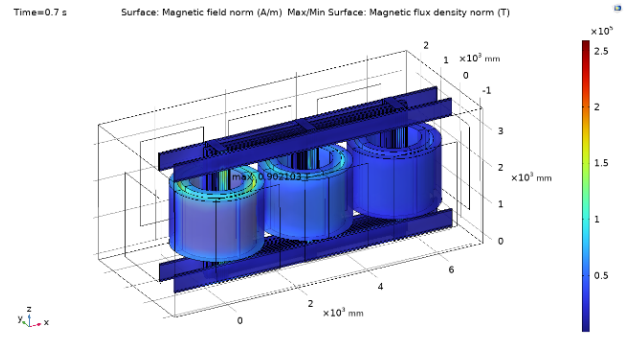
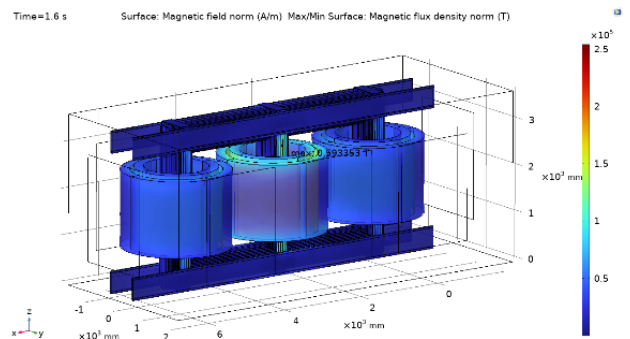


Fig. 28. Maximum magnetic flux density norm in phase a (t=0.7s)



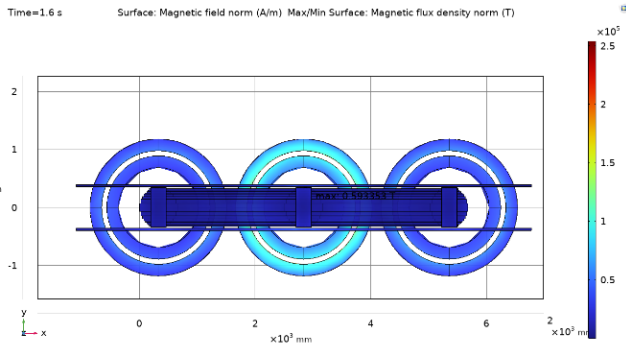


Fig. 29. Maximum magnetic flux density norm in phase b (t=1.6 s)

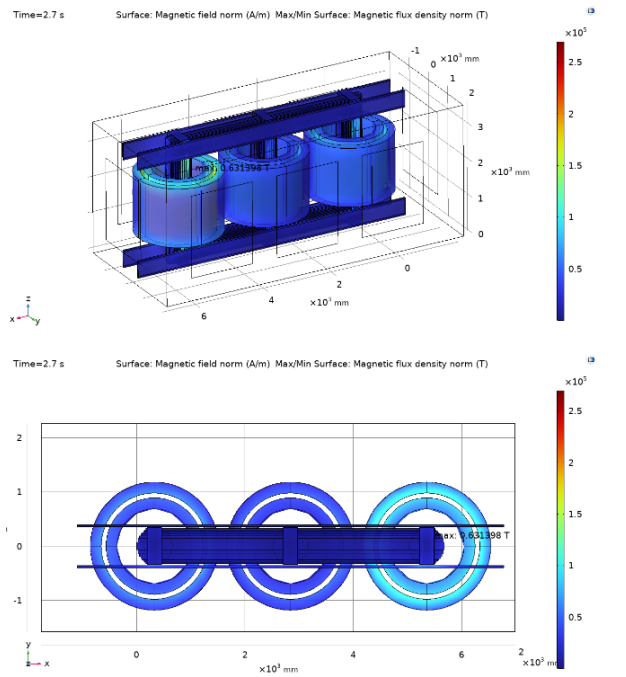


Fig. 30. Maximum magnetic flux density norm in phase c (t=2.7s)

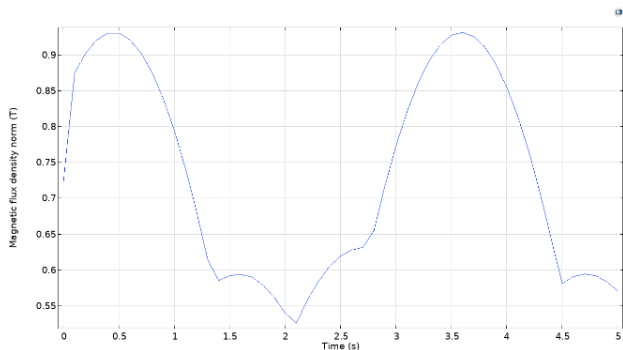


Fig. 31. Maximum magnetic flux density norm

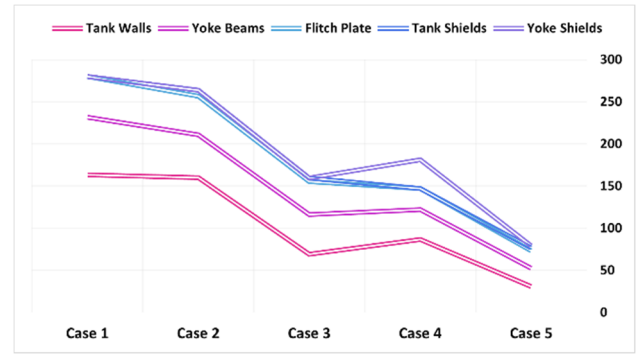


Fig. 32. Stray loss changing trends

Given that the source of leakage flux is the windings of the transformer, these critical points are located above the windings on each leg of the transformer. Each of the extreme points from a complete cycle of the graph corresponds to one phase, and at the peak point of each phase, the magnitude and distribution of the magnetic field are illustrated in Figures 28 to 32.

Table III. Stray losses in different combinations of shields

Case	1	2	3	4	5
$P_{tank\ walls}$ (kW)	163.5	160	69.2	86.7	30.7
$P_{yoke\ beams}$ (kW)	68	50.7	47.2	35.4	22
$P_{flitch\ plates}$ (kW)	48.5	45.8	39	25	20.8
$P_{tank\ shields}$ (kW)	-	7.4	4	-	3
$P_{yoke\ shields}$ (kW)	-	-	-	34	2.7
$P_{total}$ (kW)	280	263.9	159.4	181.1	79.2

### 5. CONCLUSION

Given that reducing stray losses in power transformers is important for improving efficiency, a comparative study of five combinations of shield placement was presented to reduce the stray loss effectively. Placement of the yoke shields perpendicular to the yoke beams was used to absorb high-density leakage fluxes at the top and bottom of the winding. Using these simultaneously with the tank shields, decreased the total stray loss from 280kW to 79kW, while the manufacturing cost increased.

### LIST OF SYMBOLS

- $E$  electric field (V/m)
- $D$  electric displacement (C/m<sup>2</sup>)
- $H$  magnetic field (A/m)
- $B$  magnetic field density (T)
- $\rho$  charge density (C/m<sup>2</sup>)
- $J$  current density (A/m<sup>2</sup>)
- $\sigma$  skin depth (m)
- $\delta$  conductivity (S/m)
- $\omega$  angular frequency (2\*pi\*f) (rad/s)
- $\epsilon_r$  relative permittivity (1)

$\epsilon_0$	permittivity of free space ( $F/m$ )
$\mu_r$	relative permeability (1)
$\mu_0$	permeability of free space ( $H/m$ )
$\mu''$	complex magnetic permeability ( $H/m$ )
$E_s$	source electric field ( $V/m$ )
$Q_e$	electromagnetic (EM) heating source ( $J$ )
$Q_{rh}$	heating due to induced currents ( $J$ )
$Q_{ml}$	heating due to magnetic losses ( $J$ )

## REFERENCES

- [1] L. Kralj and D. Miljavec, "Stray losses in power transformer tank walls and construction parts," in 19th International Conference on Electrical Machines, ICEM 2010, 2010. doi: 10.1109/ICELMACH.2010.5607891
- [2] S. Dasara and V. P. Mishra, "Shielding measures of power transformer to mitigate stray loss and hot spot through coupled 3D FEA," High Volt., vol. 2, no. 4, 2017, doi: 10.1049/hve.2016.0090.
- [3] C. C. Adalja and M. L. Jain, "Analysis of Stray Losses in Power Transformers by 3-D Magnetic Field Simulation," Flux, no. December, pp. 498–503, 2008.
- [4] J. Faiz, M. Ghazizadeh, and H. Oraee, "Derating of transformers under non-linear load current and non-sinusoidal voltage - An overview," IET Electr. Power Appl., vol. 9, no. 7, 2015, doi: 10.1049/iet-epa.2014.0377.
- [5] M. Eslamian and N. Mousavi, "Reduction of additional losses of power transformer using magnetic shield by 3D FEM analysis," 28th Iranian Conference on Electrical Engineering (ICEE) Tabriz, Iran.2020. pp. 762-769.
- [6] B. A. Thango and P. N. Bokoro, "Stray Load Loss Valuation in Electrical Transformers: A Review," Energies, vol. 15, no. 7. 2022. doi: 10.3390/en15072333.
- [7] L. Štrac, "Three-Phase Shunts for Stray Magnetic Field," in Procedia Engineering, 2017, vol. 202. doi: 10.1016/j.proeng.2017.09.706.
- [8] M. Moghaddami, A. I. Sarwat, and F. De Leon, "Reduction of Stray Loss in Power Transformers Using Horizontal Magnetic Wall Shunts," IEEE Trans. Magn., vol. 53, no. 2, 2017, doi: 10.1109/TMAG.2016.2611479.
- [9] S. Magdaleno-Adame, T. D. Kefalas, A. Fakhrahar, and J. C. Olivares-Galvan, "Comparative study of grain-oriented and non-oriented electrical steels in magnetic shunts of power transformers," in 2018 IEEE International Autumn Meeting on Power, Electronics and Computing, ROPEC 2018, 2019. doi: 10.1109/ROPEC.2018.8661396.
- [10] M. A. Tsili, A. G. Kladas, P. S. Georgilakis, A. T. Souflaris, and D. G. Paparigas, "Geometry optimization of magnetic shunts in power transformers based on a particular hybrid finite-element boundary-element model and sensitivity analysis," IEEE Trans. Magn., vol. 41, no. 5, 2005, doi: 10.1109/TMAG.2005.846075.
- [11] W. C. Chang, C. C. Kuo, W. C. Lin, and M. N. Hsieh, "Simulation of Stray and Core Shielding Loss for Power Transformer Based on 2D/3D FEM," IEEE Access, vol. 11, 2023, doi: 10.1109/ACCESS.2023.3242975.
- [12] Taghilou, Mahsa and Mirsalim, Mojtaba and Eslamian, Morteza and Teymouri, Ashkan, "Comparative Study of Shield Placement to Mitigate the Stray Loss of Power Transformers Based on 3D-FEM Simulation," IEEE, 2023 3rd International Conference on Electrical Machines and Drives (ICEMD), 2023. doi: 10.1109/ICEMD60816.2023.10429239